

# Vasoreactivity and peri-infarct hyperintensities in stroke

P. Zhao, PhD  
D.C. Alsop, PhD  
A. AbdulJalil, PhD  
M. Selim, MD  
L. Lipsitz, MD  
P. Novak, MD, PhD  
L. Caplan, MD  
K. Hu, PhD  
V. Novak, MD, PhD

Address correspondence and reprint requests to Dr. Vera Novak, Division of Gerontology, Beth Israel Deaconess Medical Center, 110 Francis Street, Boston, MA 02215  
vnovak@bidmc.harvard.edu

## ABSTRACT

**Objective:** It is unknown if impaired cerebral vasoreactivity recovers after ischemic stroke, and whether it compromises perfusion in regions surrounding infarct and other vascular territories. We investigated the regional differences in CO<sub>2</sub> vasoreactivity (CO<sub>2</sub>VR) and their relationships to peri-infarct T2 hyperintensities (PIHs), chronic infarct volumes, and clinical outcomes.

**Methods:** We studied 39 subjects with chronic large middle cerebral artery territory infarcts and 48 matched controls. Anatomic and three-dimensional continuous arterial spin labeling imaging at 3-Tesla MRI were used to measure regional cerebral blood flow (CBF) and CO<sub>2</sub>VR during normocapnia, hypercapnia, and hypocapnia in main arteries distributions.

**Results:** Stroke patients showed a significantly lower augmentation of blood flow at increased CO<sub>2</sub> but greater reduction of blood flow with decreased CO<sub>2</sub> than the control group. This altered vasoregulatory response was observed both ipsilateral and contralateral to the stroke. Lower CO<sub>2</sub>VR on the stroke side was associated with PIHs, greater infarct volume, and worse outcomes. The cases with PIHs (n = 27) had lower CBF during all conditions bilaterally (p < 0.0001) compared to cases with infarct only.

**Conclusions:** Perfusion augmentation is inadequate in multiple vascular territories in patients with large artery ischemic infarcts, but vasoconstriction is preserved. Peri-infarct T2 hyperintensities are associated with lower blood flow. Strategies aimed to preserve vasoreactivity after an ischemic stroke should be tested for their effect on long-term outcomes. *Neurology*® 2009;72:643-649

## GLOSSARY

**ACA** = anterior cerebral artery; **ADC** = apparent diffusion coefficient; **BP** = blood pressure; **CASL** = continuous arterial spin labeling; **CBF** = cerebral blood flow; **CO<sub>2</sub>VR** = CO<sub>2</sub> vasoreactivity; **DWI** = diffusion-weighted image; **FLAIR** = fluid-attenuated inversion recovery; **FOV** = field of view; **GM** = gray matter; **LDL** = low-density lipoprotein; **MCA** = middle cerebral artery; **MP-RAGE** = magnetization prepared rapid gradient echo; **mRS** = modified Rankin Scale; **NIHSS** = NIH Stroke Scale; **PCA** = posterior cerebral artery; **PIHs** = peri-infarct T2 hyperintensities; **TE** = echo time; **TI** = inversion time; **TR** = repetition time; **WBC** = white blood cell; **WM** = white matter.

Perfusion in regions surrounding ischemic areas is associated with recovery.<sup>1</sup> Cerebral vasoregulation maintains steady cerebral blood flow (CBF) in response to changes in CO<sub>2</sub>, but systemic blood pressure (BP) is compromised by microvascular disease and further impaired by stroke.<sup>2</sup> It is not known whether cerebral vasoregulation recovers in older people with ischemic stroke or whether vascular beds in the infarcted hemisphere remain challenged to maintain perfusion. Unrecognized brain infarctions and peri-infarct hyperintensities (PIHs) are common MRI findings during later stages after stroke.<sup>3</sup> It is unknown if the distribution of impaired vasoreactivity extends beyond the infarct region into surrounding gray and white matter and compromises perfusion in other vascular territories and regions distant from the infarct site. Continuous arterial spin labeling (CASL) MRI offers a noninvasive method to measure distribution of perfusion and vasoreactivity.<sup>4,5</sup>

From the Departments of Medicine (P.Z., K.H., V.N.), Radiology (D.C.A.), and Neurology (M.S., L.C.), Beth Israel Deaconess Medical Center, Boston; Department of Radiology (A.A.), Ohio State University, Columbus; Institute for Aging Research (L.L.), Hebrew SeniorLife, Boston, MA; and Department of Neurology (P.N.), University of Massachusetts, Boston.

Supported by American Diabetes Association 1-06-CR-25, NIH-National Institute of Neurological Disorders and Stroke R01-NS045745, NIH-National Institute of Neurological Disorders and Stroke STTR 1R41NS053128-01A2 grants to V. Novak; an NIH Older American Independence Center Grant 2P60 AG08812 and NIH Program Project P01-AG004390 to L. Lipsitz; and a General Clinical Research Center (GCRC) Grant MO1-RR01302. Dr. Lipsitz holds the Irving and Edyth S. Usen and Family Chair in Geriatric Medicine at Hebrew SeniorLife.

*Disclosure:* The authors report no disclosures.

We investigated regional differences in cerebral vasoregulation using CASL MRI at 3 Tesla to determine the long-term impact of ischemic stroke on CBF regulation and outcomes in older patients.

A better understanding of post-stroke CBF regulation may have significant impact on outpatient management, e.g., blood pressure control for optimal cerebral blood perfusion, and future studies of poststroke recovery.

**METHODS Subjects.** Studies were conducted in the Syncope and Falls in the Elderly Laboratory and at the Magnetic Resonance Imaging Center at Beth Israel Deaconess Medical Center. The stroke patient group consisted of 39 subjects with chronic large artery hemispheric middle cerebral artery (MCA) infarcts documented on MRI or CT during the acute phase,  $6.3 \pm 5.8$  years after stroke, and clinically stable. Neurologic and functional outcomes of stroke patients were assessed by NIH Stroke Scale (NIHSS) and Modified Rankin Scale (mRS). We screened control subjects based on the running average of the stroke patients and we recruited 48 age-, sex-, and hypertension-matched controls, with no clinical history of stroke and no focal deficits on neurologic examination. Twenty-five stroke and 17 nonstroke participants were treated for hypertension. We excluded subjects with intracranial or subarachnoid hemorrhage on MRI or CT, diabetes mellitus, clinically significant arrhythmias, severe hypertension (systolic BP >200 or diastolic BP >110 mm Hg or subjects taking three or more antihypertensive medications), morbid obesity, carotid stenosis >50% for the control and on the nonstroke side for the cases, any metallic bioimplants, and claustrophobia. Intracranial stenosis was not an exclusion in the study because it may play a role in pathophysiology of large vessel stroke. Antihypertensive medications were tapered and withdrawn for 3 days before the study, in order to reduce the acute effects of antihypertensive medications on CBF. Laboratory chemistries included routine blood, glucose, lipid, and renal panels, differential white blood cell count, and urine chemistry panel.

**MRI.** All MRI studies were performed on a 3-Tesla GE Signa Vhi or Excite MRI scanner using a quadrature and phase array head coils (GE Medical Systems, Milwaukee, WI). High-resolution anatomic images include three-dimensional magnetization prepared rapid gradient echo (MP-RAGE) (repetition time [TR]/echo time [TE]/inversion time [TI] = 7.8/3.1/600 msec, 3.0 mm slice thickness, 52 slices, bandwidth = 122 Hz per pixel, flip angle = 10°, 24 cm × 24 cm field of view [FOV], 256 × 192 matrix size), fluid-attenuated inversion recovery (FLAIR) (TR/TE/TI = 11,000/161/2,250 msec, 5 mm slice thickness, 30 slices, bandwidth = 122 Hz per pixel, flip angle = 90°, 24 cm × 24 cm FOV, 256 × 160 matrix size), and diffusion-weighted image (DWI) (b value of 1,000 seconds/mm<sup>2</sup>, TR/TE = 10,000/86.6 msec, 5 mm slice thickness, bandwidth = 250 kHz, 128 × 128 matrix size). CASL is sensitive to the CBF change and can be used for noninvasive mapping of CBF (mL · 100 g<sup>-1</sup> · min<sup>-1</sup>) and vasoreactivity.<sup>4,6,7</sup> CASL images were acquired using a custom three-dimensional stack of interleaved spirals fast spin echo sequence (TR/TE = 6,000/23.8 msec, echo train length = 66, with a 18 × 18 cm FOV, in the coronal plane and 64 slices with thickness = 3.8 mm, eight spiral interleaves, two averages and a bandwidth = ±62.5 kHz).

**Imaging protocol.** Labeled and unlabeled images were collected over 2-minute periods during normal breathing (four scans), CO<sub>2</sub> rebreathing with 95% air and 5% CO<sub>2</sub>, and hyperventilation (two scans each). Quantitative CBF data were reconstructed for each condition<sup>4,7</sup> using custom software written in interactive data language (IDL) (Research Systems, Boulder, CO). End-tidal CO<sub>2</sub> was continuously monitored and averaged over 15-second intervals for all conditions. During hyperventilation, end-tidal pCO<sub>2</sub> was monitored and the subject was instructed to alter breathing rate to maintain an approximate pressure of 25 mm Hg. BP was measured in 1-minute intervals.

**Image analysis.** All image data were automatically saved to a CD-RW attached to the scanner. The data were analyzed on a Linux workstation using tools developed in IDL. Infarcts were outlined on T2-weighted and FLAIR images. PIHs were defined as hyperintense areas adjacent to the infarcts on T2-weighted and FLAIR images and hyperintensities on DWI, and were quantified on FLAIR images. MP-RAGE images were used to quantify volume of white matter (WM), gray matter (GM), and CSF by an inherently circular model in statistical parametric mapping software package (SPM, University College London, UK) involving spatial normalization and tissue classification.<sup>8</sup> A rigid-body model<sup>9,10</sup> was used for coregistration of MP-RAGE, FLAIR, and CASL images. A template of the three primary vascular distributions was applied to measure perfusion in the anterior cerebral artery (ACA), middle cerebral artery (MCA), and posterior cerebral artery (PCA) territories.<sup>11</sup>

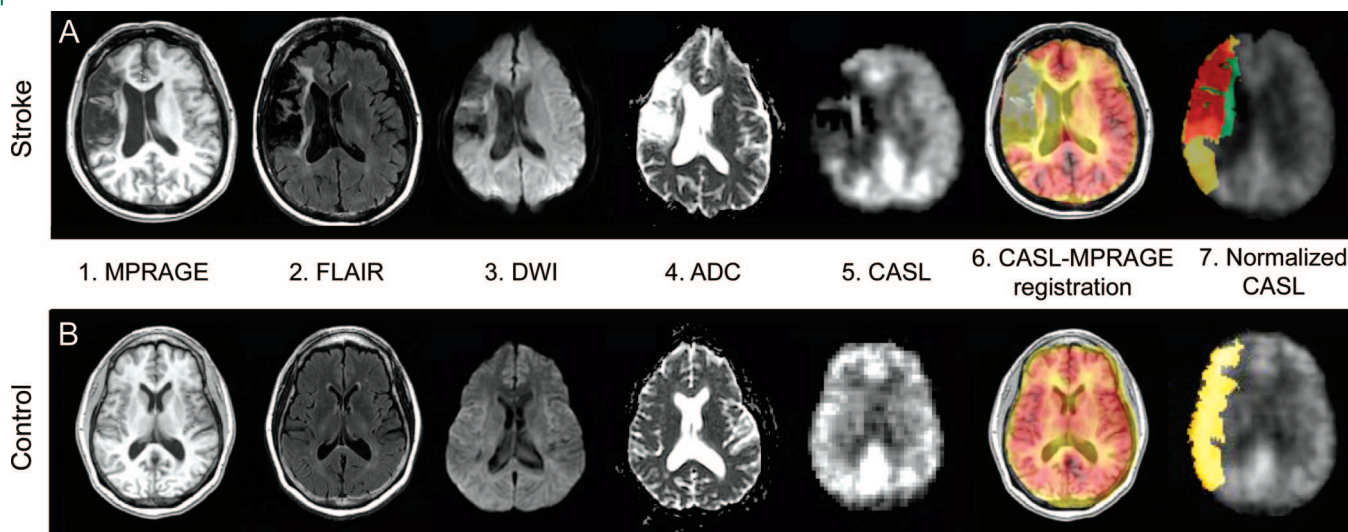
Figure 1 is an example of perfusion image registration on anatomic images for a subject with right MCA territory infarctions (A) and a control (B). The perfusion CASL image<sup>5</sup> and anatomic MP-RAGE image<sup>1</sup> are coregistered<sup>6</sup> and normalized to standard template.<sup>7</sup> The infarct (red) and PIHs (green) on the structural images,<sup>1,2</sup> DWI,<sup>3</sup> and apparent diffusion coefficient (ADC) map derived from DWI<sup>4</sup> and MCA territory (yellow) are normalized and overlaid on normalized CASL.<sup>7</sup>

Several indices of response to CO<sub>2</sub> modulations were calculated. The slope of the regression between CBF and CO<sub>2</sub>, in units of mL/100 g/min/mm Hg, is referred to as the cerebral vasoreactivity (CO<sub>2</sub>VR). We have assessed separately the vasodilation response or ability to augment flow during rebreathing (CO<sub>2</sub>VR<sub>Base-RB</sub>) and vasoconstriction response or flow reduction during hyperventilation (CO<sub>2</sub>VR<sub>Base-HV</sub>) using same approach. Relative CO<sub>2</sub>VR reflects the fractional change in CBF and CO<sub>2</sub> compared to baseline.

**Statistical analysis.** Statistical analysis was conducted by Vera Novak and Peng Zhao. Descriptive statistics were used to summarize all variables. Demographic and laboratory variables were compared between the stroke and control groups using one-way analysis of variance and Fisher exact test. The volumes of normalized WM, GM, and CSF were compared between the groups using the least-square models with adjustments for age and sex. In the stroke group, perfusion was compared between the stroke side (22 right, 17 left hemisphere) and nonstroke side for each vascular territory. In the control group, perfusion values were randomized between the right and left hemispheres to match the percentage distribution of infarcts in each hemisphere in the stroke group. For example, perfusion on stroke side was compared to randomized side 1 (RND 1) and perfusion on nonstroke side was compared to randomized side 2 (RND 2) in the control group.

CBF and CO<sub>2</sub>VR were compared between the groups using the least-square models and two-way multivariate analysis of variance with adjustments for age, sex, infarct side, and RND side 1 and 2, and vascular territories. The effects of infarct vol-

**Figure 1** Anatomic and perfusion MR images



Example of perfusion image registration on anatomic images for a subject with right middle cerebral artery (MCA) territory infarctions (A) and a control (B). The perfusion continuous arterial spin labeling (CASL) image (5) and anatomic magnetization prepared rapid gradient echo (MP-RAGE) image (1) are coregistered (6) and normalized to standard template (7). The infarct (red) and peri-infarct T2 hyperintensities (green) on the structural images (1, 2), diffusion-weighted image (DWI) (3), and apparent diffusion coefficient (ADC) map derived from DWI (4) and MCA territory (yellow) are normalized and overlaid on normalized CASL (7). FLAIR = fluid-attenuated inversion recovery.

ume, systolic blood pressure, hypertension, NIHSS, and mRS were assessed using the same approaches.

**RESULTS Demographic and laboratory measures.** A total of 172 subjects were screened consecutively and provided informed consent, approved by the Institutional Review Board; 87 subjects completed the protocol study and MRI scanning. Table 1 presents the demographic characteristics, brain volumes, blood pressure, and laboratory results for the stroke and control groups that were similar, except for CSF volume ( $p = 0.0005$ ), low-density lipoprotein ( $p = 0.02$ ), and total cholesterol ( $p = 0.01$ ).

**Cerebral blood flow.** Figure 2 shows CBF in the ACA (A1), MCA (A2), and PCA (A3) territories during baseline, CO<sub>2</sub> rebreathing, and hyperventilation for the stroke and control groups. In the stroke group, CBF on the stroke side was lower than in the control group in the MCA territory during baseline ( $p = 0.03$ ) and in all territories during CO<sub>2</sub> rebreathing ( $p < 0.0007$ ) and hyperventilation ( $p < 0.03$ ). On the nonstroke side, CBF was lower during CO<sub>2</sub> rebreathing in ACA ( $p = 0.01$ ) and PCA ( $p = 0.03$ ) territories and borderline in the MCA territory ( $p = 0.07$ ). Within the stroke group, CBF was lower on the stroke side than the nonstroke side during all conditions and across all territories ( $p < 0.0015$ ).

**CO<sub>2</sub> vasoreactivity.** Table 2 summarizes measures of CO<sub>2</sub>VR and figure 2 (B1–B3) shows vasodilation and vasoconstriction responses separately. CO<sub>2</sub>VR was lower on the stroke side compared to the control group in the ACA ( $p = 0.02$ ) and MCA ( $p = 0.003$ ) territo-

ries and in all territories compared to the nonstroke side (table 2). There were no significant differences in CO<sub>2</sub>VR among the infarct slices, PIH slices, and whole brain. Flow augmentation during rebreathing was significantly reduced compared to controls and to nonstroke side. Vasodilation response (CO<sub>2</sub>VR<sub>Base-RB</sub>) was lower on the stroke side compared to control group in all territories (figure 2, B1–B3) and was also lower on the nonstroke side in ACA ( $p = 0.008$ ) and MCA ( $p = 0.03$ ) territories. Within the stroke group, vasodilation response was lower on the stroke side than the nonstroke side in ACA ( $p = 0.002$ ) and MCA ( $p = 0.01$ ) territories. In contrast, flow reduction during hyperventilation was preserved. Vasoconstriction response (CO<sub>2</sub>VR<sub>Base-HV</sub>) was greater in the stroke group compared to the control group on both sides. Within the stroke group, CO<sub>2</sub>VR<sub>Base-HV</sub> was lower on the stroke side than the nonstroke side in all territories.

Similarly, the relative vasodilation and vasoconstriction responses were consistently different between the groups. Within the stroke group, however, there were no significant differences in the relative reactivity between stroke and nonstroke sides. BP did not significantly change between conditions. CO<sub>2</sub>VR was not significantly associated with BP change between conditions.

**CBF, CO<sub>2</sub>VR, and outcomes.** The larger infarct volume and PIH volume were both related to the higher NIHSS (infarct  $p < 0.0001$ ,  $r = 0.7$ , PIH  $p = 0.005$ ,  $r = 0.57$ ) and mRS (infarct  $p < 0.0001$ ,  $r = 0.7$ , PIH  $p = 0.001$ ,  $r = 0.67$ ). In the stroke group, lower baseline CBF on stroke side was associated

**Table 1** Demographic characteristics and laboratory results

Group	Stroke	Control	p
Age, y	64.5 ± 8.8	67.8 ± 7.0	NS
Male/female	19/20	21/27	NS
Race (W/A/AI/AA/U)	33/1/0/5/0	39/3/1/4/1	NS
Body mass index (kg/m <sup>2</sup> )	27.5 ± 4.7	25.8 ± 4.0	NS
Systolic BP (mm Hg)	129.9 ± 15.3	124.1 ± 15.0	NS
Diastolic BP (mm Hg)	60.6 ± 9.3	60.3 ± 9.6	NS
Years after stroke	6.3 ± 5.8 (0.5-30)	—	—
Stroke side (right/left)	22/17	—	—
Infarct volume (cm <sup>3</sup> )	20.3 ± 35.1	—	—
PIH volume (cm <sup>3</sup> )	20.2 ± 18.9	—	—
WM volume (cm <sup>3</sup> )	416.7 ± 72.4	422.5 ± 51.4	NS
GM volume (cm <sup>3</sup> )	614.6 ± 12.0	625.8 ± 10.8	NS
CSF volume (cm <sup>3</sup> )	438.0 ± 12.0	391.9 ± 10.8	0.005
NIHSS	2.7 ± 2.7 (0-10)	—	—
mRS	1.3 ± 1.2 (0-4)	—	—
WBC count (k/ $\mu$ L)	7.1 ± 2.2	6.5 ± 1.7	NS
Hemoglobin (g/dL)	13.7 ± 0.2	13.8 ± 0.2	NS
Hematocrit (%)	40.2 ± 3.6	40.5 ± 3.4	NS
Cholesterol (mg/dL)	179.7 ± 40.8	201.8 ± 38.4	0.01
LDL (mg/dL)	94.0 ± 33.1	111.5 ± 32.3	0.02
Triglycerides (mg/dL)	135.0 ± 76.5	145.7 ± 75.0	NS

Continuous variables are presented as mean  $\pm$  SD; ordinal variables are presented as mean  $\pm$  SD (range); nominal variables are presented as numbers.

NS = comparison is not significantly different if  $p > 0.05$ ; W = White; A = Asian; AI = American Indian; AA = African American; U = unknown; BP = blood pressure; PIH = peri-infarct T2 hyperintensities; WM = white matter; GM = gray matter; NIHSS = NIH Stroke Scale; mRS = modified Rankin Scale; WBC = white blood cell; LDL = low-density lipoprotein.

with greater infarct volume and PIH volumes (infarct  $p < 0.0001$ ,  $r = 0.64$ ; PIH  $p < 0.0001$ ,  $r = 0.66$ ) and worse outcomes (NIHSS  $p = 0.018$ ,  $r = 0.45$  and mRS  $p < 0.0001$ ,  $r = 0.49$ ). Higher baseline CBF indicated less atrophy in both groups, i.e., greater GM volume (stroke  $p = 0.006$ ,  $r = 0.46$ ) and smaller CSF volume (control  $p = 0.002$ ,  $r = 0.49$ , stroke  $p = 0.03$ ,  $r = 0.45$ ). Lower CO<sub>2</sub>VR on the stroke side was associated with greater infarct ( $p = 0.01$ ,  $r = 0.48$ ) and PIH ( $p = 0.0006$ ,  $r = 0.48$ ) volumes, higher mRS ( $p = 0.03$ ,  $r = 0.48$ ), and higher systolic ( $p = 0.008$ ,  $r = 0.48$ ) and diastolic blood pressures ( $p < 0.0001$ ,  $r = 0.52$ ).

**Peri-infarct T2 hyperintensities.** Figure 1 A7 shows the PIHs area in green. Twenty-seven patients had both infarcts and PIHs and 12 patients had only infarcts. The cases with PIHs were older than cases without PIHs ( $68.8 \pm 2.4$  vs  $62.6 \pm 1.6$  years old,  $p = 0.04$ ), had greater total infarct and PIH lesions volumes ( $47.63 \pm 56.85$  vs  $4.41 \pm 3.48$  cm<sup>3</sup>,  $p = 0.013$ ), lower CBF during all conditions bilaterally ( $p < 0.0001$ ), and borderline lower CO<sub>2</sub>VR on the

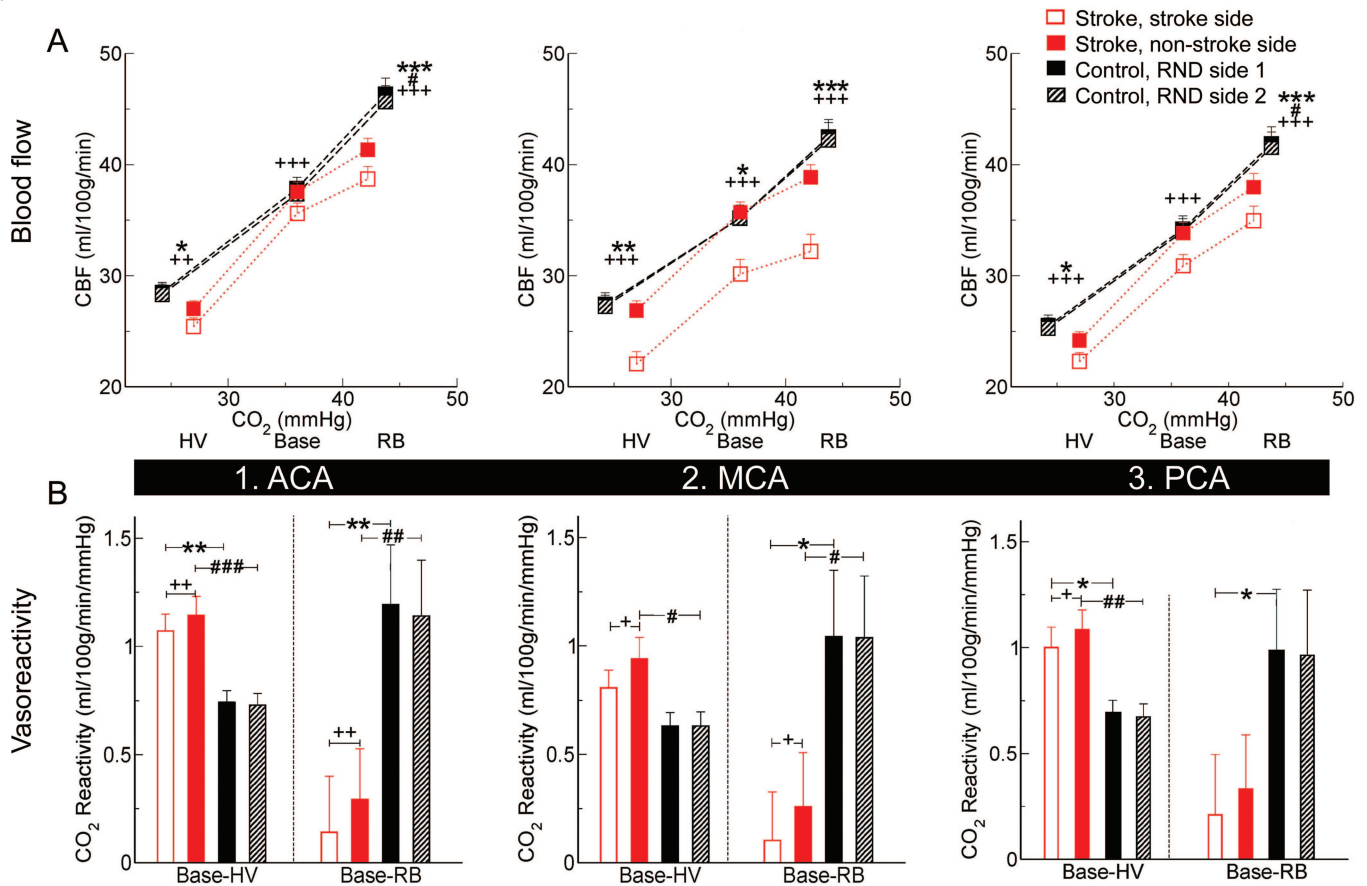
stroke side ( $p = 0.07$ ). There was a tendency for worse outcomes in PIH cases (NIHSS  $3.15 \pm 0.5$  vs  $1.8 \pm 0.77$ ,  $p = 0.17$ ; mRS  $1.4 \pm 0.2$  vs  $0.9 \pm 0.35$ ,  $p = 0.24$ ) but it did not reach significance.

**DISCUSSION** This study showed that baseline perfusion and perfusion augmentation in response to CO<sub>2</sub> challenge are chronically reduced after ischemic stroke. Distribution of impaired reactivity extends beyond the infarct area into other major vascular territories and regions distant from the infarct site. Both hemispheres were affected by vasodilation impairment. Perfusion reserve was only 9% in the infarcted and 10% in the noninfarcted hemispheres, compared to 24% reserve in the control group. In contrast, vasoconstriction reserve (>23%) was normal, and the rate of vasoconstriction was even exaggerated. Since vasodilation is the capability to augment flow in a challenge, the impairment in vasodilation reactivity is of particular importance. In the control group, vasodilation increased linearly over the physiologic CO<sub>2</sub> range (figure 2, A1–A3). In the stroke group, the vasoreactivity response was nonlinear with a greater blood flow reduction with decreased CO<sub>2</sub>, but weaker rise with increasing CO<sub>2</sub>. This observation motivated the separate analysis of vasoconstriction and vasodilation reserves. These findings suggest that baseline perfusion in the infarcted territory is maintained near maximum reserve capacity, possibly through collateral flow and dilatation of small vessels.

Previous studies reported regional differences in perfusion<sup>12</sup> with normal<sup>13</sup> or chronically reduced vasoreactivity.<sup>14</sup> Reduced vasomotor reserve in the affected hemisphere was also associated with worsening of acute neurologic status poststroke.<sup>15</sup> Elevated oxygen extraction fraction and reduced blood flow and vasoreactivity had impact on long-term prognosis and risk for future strokes in patients with carotid occlusive disease.<sup>16</sup>

Peri-infarct hyperintensities are common findings on DWIs during subacute and later stages of stroke, but their relationship to CBF maps has received less attention. PIH lesions are typically within white matter, are larger than isointense lesions, and their distribution may extend into other vascular territories. Increased T2 signal intensity during the chronic phase is attributed to prolonged T2-relaxation time and cellular edema. The mechanisms underlying this phenomenon are not well understood. T2 hyperintensities may indicate a delayed or impaired repair of ischemic tissue and impairments of flow in microvessels.<sup>17</sup> Disruption of blood–brain barrier, accompanied by extravasation of fluid and tissue swelling, may extend into areas of gray and white matter sur-

**Figure 2** Perfusion and vasoreactivity



The top panel shows perfusion in main vascular territories anterior cerebral artery (ACA) (A1), middle cerebral artery (MCA) (A2), and posterior cerebral artery (PCA) (A3) during hyperventilation (HV), baseline (Base), and CO<sub>2</sub> rebreathing (RB) conditions for the stroke group and control group. The bottom panel shows vasoreactivity to CO<sub>2</sub> challenges in the same territories ACA (B1), MCA (B2), and PCA (B3). On the left it is vasoconstriction reactivity between baseline and hyperventilation (Base-HV), and on the right it is vasodilation reactivity between baseline and CO<sub>2</sub> rebreathing (Base-RB). Stroke group: stroke side, nonstroke side; control group: randomized side 1, i.e., RND side 1, randomized side 2, i.e., RND side 2. \*Stroke side vs control RND side 1, #nonstroke side vs control RND side 2, +stroke side vs nonstroke side within stroke group. \*\*\* or ### or +++ means  $p < 0.0009$ , \*\* or ## or ++ means  $0.001 < p < 0.009$ , \* or # or + means  $0.01 < p < 0.05$ .

rounding the infarct and affect regions distant from the infarct site. Our study linked PIHs with abnormal vasoreactivity, and provided evidence that T2 hyperintensities are associated with the final infarct volume and neurologic outcomes. Distributions of impaired vasoreactivity and PIHs were similar and extended into other vascular territories and non-infarcted hemisphere.

Our results may have implications for therapies directed at improvement of vasoreactivity and perfusion. Recently, it was shown that impaired vasoreactivity can be improved using nitric oxide donors.<sup>18</sup> If effective, this approach may be useful to facilitate perfusion recovery. Further investigations, however, are needed to identify treatment strategies for permanent improvement of vascular reactivity. Second, the observation that lower CO<sub>2</sub> vasoreactivity was associated with higher systemic BP and higher exaggerated rate of vasoconstriction may suggest interactions between CO<sub>2</sub> vasoreactivity and pressure autoregulation.

These interactions may further affect perfusion in hypertensive patients and play a role in BP management after stroke. Therefore, combined therapies that would improve endothelial reactivity may be beneficial for long-term outpatient management.

CASL has been successfully applied to assess CBF and cerebrovascular hemodynamic reserve in patients with chronic cerebrovascular disease.<sup>4,5</sup> CASL measures of cerebral perfusion are highly accurate in detecting lesion laterality in temporal lobe epilepsy, stenotic-occlusive disease, and brain tumors.<sup>19,20</sup> Among patients with cerebrovascular disease, CASL CBF has excellent concurrent validity when correlated with CBF measured by positron emission tomography<sup>21,22</sup> or with dynamic susceptibility-weighted magnetic resonance.<sup>19</sup> A correlative study of CASL with CO<sub>2</sub> PET validation demonstrated that quantification of CBF using CASL is feasible and reasonable in patients with chronic occlusive cerebrovascular disease, even when employed in a rou-

**Table 2** Measurements of cerebral vasoreactivity and vasomotor reserve

Vasoregulation	Group	Hemisphere	ACA territory	MCA territory	PCA territory
CO <sub>2</sub> VR (mL/100 g/min/mm Hg)	Stroke	Stroke side	0.77 ± 0.39 <sup>***</sup>	0.58 ± 0.36 <sup>***</sup>	0.73 ± 0.37 <sup>#</sup>
		Nonstroke side	0.83 ± 0.40	0.68 ± 0.35	0.80 ± 0.36
	Control	RND side 1	0.89 ± 0.39	0.75 ± 0.35	0.82 ± 0.35
		RND side 2	0.87 ± 0.38	0.76 ± 0.35	0.82 ± 0.35
% CBF augmentation	Stroke	Stroke side	11 ± 17 <sup>***</sup>	9 ± 15 <sup>***</sup>	12 ± 19 <sup>***</sup>
		Nonstroke side	12 ± 15 <sup>***</sup>	10 ± 13 <sup>***</sup>	12 ± 17 <sup>***</sup>
	Control	RND side 1	26 ± 24	24 ± 23	28 ± 25
		RND side 2	27 ± 26	23 ± 23	29 ± 25
% CBF reduction	Stroke	Stroke side	27 ± 14	24 ± 14	27 ± 15
		Nonstroke side	26 ± 14	23 ± 14	27 ± 15
	Control	RND side 1	22 ± 15	21 ± 15	23 ± 15
		RND side 2	22 ± 16	21 ± 15	23 ± 16

\*Comparison between the stroke side and control RND side 1.

\*Comparison between the nonstroke side and control RND side 2.

#Comparison between stroke side and nonstroke side within stroke group.

Three symbols \*\*\* or \*\* or # denotes  $p < 0.0009$ , \*\* or \* or # denotes  $0.001 < p < 0.009$ , and \* or + or # denotes  $0.01 < p < 0.05$ .

ACA = anterior cerebral artery; MCA = middle cerebral artery; PCA = posterior cerebral artery; CO<sub>2</sub>VR = CO<sub>2</sub> vasoreactivity; % CBF augmentation = the percent CBF increase above baseline; % CBF reduction = the percent CBF decrease below baseline.

tine clinical setting. The long transit time, however, may lead to CBF underestimation on the occluded side. In our study, CASL may have underestimated perfusion at low flow states, such as hypocapnia, due to the short decay time of the CASL label (~1 s), and therefore it is possible that the perfusion deficit during hypocapnia may be even greater.

A cross-sectional study design, with a modest sample size and specific inclusion criteria, may pose some limitations for data interpretation. With this design, we cannot exclude the possibility that impaired vasoreactivity was present even before the stroke due to a strong coupling between reactivity and stroke risk. However, we were careful to match the controls to stroke patients with a similar distribution of vascular risks, BP, and age. To provide better matched groups, we excluded patients with bad outcomes, large infarcts, and diabetes, who may have even more severe perfusion deficit and endothelial dysfunction. A consequence of our careful matching is that in general population with other comorbidities, the vasoreactivity and flow reserve values may be even lower than measured in this select stroke patient group.

This study has shown that perfusion regulation is persistently altered in patients with chronic large artery ischemic infarcts, and that distribution of impaired vasoreactivity extends beyond the infarcted region into other vascular territories and noninfarcted hemisphere. Notably, the ability to augment flow is impaired while vasoconstriction is preserved

or elevated. PIHs are associated with vasoreactivity and with final infarct volume and clinical outcomes. The use of CASL and vasoreactivity imaging is a novel approach for identification of flow regulation that provides new information about regional differences of vasoreactivity after ischemic stroke.

## ACKNOWLEDGMENT

The authors thank Ihab Hajjar, MD, from Hebrew SeniorLife; nurses from General Clinical Research Center; Sarah LaRose, BS, and Laura DesRochers, BS, from the Division of Gerontology; and Rob Marquise, BS, Fontini Kourtelidis, BS, and Susan LaRuche, BS, from the Radiology Department, Beth Israel Deaconess Medical Center, for help with data acquisition.

Received June 20, 2008. Accepted in final form November 17, 2008.

## REFERENCES

- Nabavi DG, Cenic A, Henderson S, Gelb AW, Lee TY. Perfusion mapping using computed tomography allows accurate prediction of cerebral infarction in experimental brain ischemia. *Stroke* 2001;32:175–183.
- Derdeyn CP, Grubb RL, Powers WJ. Cerebral hemodynamic impairment: methods of measurement and association with stroke risk. *Neurology* 1999;53:251–259.
- Price TR, Manolio TA, Kronmal RA, et al. Silent brain infarction on magnetic resonance imaging and neurological abnormalities in community-dwelling older adults. *Stroke* 1997;28:1158–1164.
- Detre JA, Alsop DC, Vives LR, Maccotta L, Teener JW, Raps EC. Noninvasive MRI evaluation of cerebral blood flow in cerebrovascular disease. *Neurology* 1998;50:633–641.

5. Detre JA, Samuels OB, Alsop DC, Gonzalez-At JB, Kasner SE, Raps EC. Noninvasive magnetic resonance imaging evaluation of cerebral blood flow with acetazolamide challenge in patients with cerebrovascular stenosis. *J Magn Reson Imaging* 1999;10:870–875.
6. Alsop DC, Detre JA. Reduced transit-time sensitivity in non-invasive magnetic resonance imaging of human cerebral blood flow. *J Cereb Blood Flow Metab* 1996;16:1236–1249.
7. Alsop DC, Detre JA. Multisection cerebral blood flow MR imaging with continuous arterial spin labeling. *Radiology* 1998;208:410–416.
8. D'Agostino E, Maes F, Vandermeulen D, Suetens P. Non-rigid atlas-to-image registration by minimization of class-conditional image entropy. In: Barillot C, Haynor D, Hellier P, eds. *Medical Image Computing and Computer-Assisted Intervention—MICCAI 2004 Lecture Notes in Computer Science*. Springer-Verlag;2004:745–753.
9. Collignon A, Maes F, Delaere D, Vandermeulen D, Suetens P, Marchal G. Automated multimodality image registration based on information theory. In: Bizais Y, Barillot C, DiPaola R, eds. *Information Processing in Medical Imaging*. Dordrecht: Kluwer Academic Publishers; 1995: 263–274.
10. Wells III WM, Viola P, Atsumi H, Nakajima S, Kikinis R. Multi-modal volume registration by maximization of mutual information. *Med Image Anal* 1996;1:35–51.
11. Floyd TF, Ratcliffe SJ, Wang J, Resch B, Detre JA. Precision of the CASL-perfusion MRI technique for the measurement of cerebral blood flow in whole brain and vascular territories. *J Magn Reson Imaging* 2003;18:649–655.
12. Rodriguez G, Nobili F, De Carli F, et al. Regional cerebral blood flow in chronic stroke patients. *Stroke* 1993;24:94–99.
13. Sakashita Y, Matsuda H, Kakuda K, Takamori M. Hypoperfusion and vasoreactivity in the thalamus and cerebellum after stroke. *Stroke* 1993;24:84–87.
14. Cupini L, Diomedei M, Placidi F, Silvestrini M, Giacomini P. Cerebrovascular reactivity and subcortical infarctions. *Arch Neurol* 2001;58:577–581.
15. Alvarez FJ, Segura T, Castellanos M, et al. Cerebral hemodynamic reserve and early neurologic deterioration in acute ischemic stroke. *J Cereb Blood Flow Metab* 2004;24:1267–1271.
16. Hokari M, Kuroda S, Shiga T, Nakayama N, Tamaki N, Iwasaki Y. Impact of oxygen extraction fraction on long-term prognosis in patients with reduced blood flow and vasoreactivity because of occlusive carotid artery disease. *Surg Neurol Epub* 2008 May 29.
17. Mandell DM, Han JS, Poub Blanc J, et al. Selective reduction of blood flow to white matter during hypercapnia corresponds with leukoaraiosis. *Stroke* 2008;39:1993–1998.
18. Lavi S, Gaitini D, Milloul V, Jacob G. Impaired cerebral CO<sub>2</sub> vasoreactivity: association with endothelial dysfunction. *Am J Physiol Heart Circ Physiol* 2006;291:H1856–H1861.
19. Brown GG, Clark C, Liu TT. Measurement of cerebral perfusion with arterial spin labeling: Part 2. Applications. *J Int Neuropsychol Soc* 2007;13:526–538.
20. Wolf RL, Alsop DC, Levy-Reis I, et al. Detection of mesial temporal lobe hypoperfusion in patients with temporal lobe epilepsy by use of arterial spin labeled perfusion MR imaging. *AJNR Am J Neuroradiol* 2001;22:1334–1341.
21. Kimura H, Kado H, Koshimoto Y, Tsuchida T, Yonekura Y, Itoh H. Multislice continuous arterial spin-labeled perfusion MRI in patients with chronic occlusive cerebrovascular disease: a correlative study with CO<sub>2</sub> PET validation. *J Magn Reson Imaging* 2005;22:189–198.
22. Ye FQ, Berman KF, Ellmore T, et al. H<sub>2</sub>(15)O PET validation of steady-state arterial spin tagging cerebral blood flow measurements in humans. *Magn Reson Med* 2000;44:450–456.

## Save with Exclusive AAN Member Benefits!

Looking for the best value in home, term-life or medical malpractice insurance for you and your family? How about competitive rates on credit cards or simplified payment processing?

Enjoy these and more exclusive benefits already included with your AAN membership, in the AAN Partners Program. We've done the leg work to find the best values on quality products and services. We've negotiated these offerings so low that they could save you MORE than the cost of your membership!

Take advantage of ALL your Academy benefits today, visit [www.aan.com/pp08](http://www.aan.com/pp08) to get started!